Brillouin light storage for 100 pulse widths

Check for updates

Birgit Stiller[1,2,3] ✉, Kevin Jaksch[1,2,3], Johannes Piotrowski[4,5], Moritz Merklein[2,3], Mikołaj K. Schmidt[5], Khu Vu[6], Pan Ma[6], Stephen Madden[6], Michael J. Steel[5], Christopher G. Poulton[7] & Benjamin J. Eggleton[2,3]

Signal processing based on stimulated Brillouin scattering (SBS) is limited by the narrow linewidth of the optoacoustic response, which confines many Brillouin applications to continuous wave signals or optical pulses longer than several nanoseconds. In this work, we experimentally demonstrate Brillouin interactions at the 150 ps time scale and a delay for a record 15 ns which corresponds to a delay of 100 pulse widths. This breakthrough experimental result was enabled by the high local gain of the chalcogenide waveguides as the optoacoustic interaction length reduces with pulse width. We successfully transfer 150 ps-long pulses to traveling acoustic waves within a Brillouin-based memory setup. The information encoded in the optical pulses is stored for 15 ns in the acoustic field. We show the retrieval of eight amplitude levels, multiple consecutive pulses, and low distortion in pulse shape. The extension of Brillouin-based storage to the ultra-short pulse regime is an important step for the realization of practical Brillouin-based delay lines and other optical processing applications.

Nonlinear scattering processes such as stimulated Rayleigh, Raman, and Brillouin scattering can be distinguished in the optical domain through their different frequency shifts and spectral line widths. These parameters are characteristic of the light-matter interaction with either macroscopic or molecular vibrations[1,2]. Due to its narrow gain linewidth of several tens of MHz, stimulated Brillouin scattering (SBS) is particularly interesting for applications such as optical and microwave filters[3–7], signal processing[8–12], and narrow-linewidth lasers[13–16]. On the one hand, the narrow linewidth would suggest that only long pulses can be delayed; the time-bandwidth product then limits the fractional delay. For example, SBS-based slow-light schemes are usually limited to a delay of one or two pulse widths[17]. Zhu et al. showed SBS slow-light delay for pulses as short as 75 ps, but with a delay of less than one pulse width[18] Cascading the SBS slow-light process permits small improvements in the delay but at the cost of added system complexity[19]. To overcome these limitations, another concept that uses SBS for delaying optical signals can be used: that of "Brillouin-based memory" (BBM)[18,20], which temporarily stores information encoded in light signals as traveling acoustic waves. In these experiments, although there is no slowing of the optical pulse itself, the information can be held in a short distance for comparatively long lengths of time, because the processes of acoustic propagation and loss are five orders of magnitude slower than for optical waves. This concept has been demonstrated in highly nonlinear fibers and integrated photonic circuits[18,20] for nanosecond pulses with a storage time of 10 nanoseconds, limited by the acoustic lifetime. The storage can operate at

room temperature and can simultaneously store multiple signals that are closely spaced in frequency without significant cross-talk[21]. In ref. [20], both an enhancement of the operating bandwidth towards the GHz regime and the ability to store and retrieve coherent information were demonstrated. Further work showed the non-reciprocity and cascading of the process[22,23], as well as dynamic reinforcement of the acoustic waves[24]. However, so far experiments in BBM (as well as in many other Brillouin phenomena), have been limited to nanosecond-long optical pulses[25].

In this work, we experimentally demonstrate the optoacoustic storage of pulses as short as 150 ps for up to 15 ns corresponding to 100 pulse widths, using the BBM technique. We achieve storage of pulses with a linewidth that exceeds the Brillouin linewidth by two orders of magnitude, from 30 MHz to about 3 GHz. The giant Brillouin gain of highly nonlinear chalcogenide waveguides enables highly efficient storage of such short pulses within cm-scale waveguides so that the pulse shapes are not significantly affected by dispersion; we store and retrieve eight different power levels while maintaining pulse width and shape. The acoustic lifetime is herein not altered because the intrinsic Brillouin spectrum remains unchanged; the short pulse storage is instead enabled by the large Brillouin gain. For pulses with a pulse duration shorter than one nanosecond, we observe a complex behavior of the read-out efficiency oscillating as a function of the delay time. We discuss several possible mechanisms for this observation: (i) the reach of a transient regime for pulses shorter than 1 ns that is not well described by the usual approximations made in the coupled
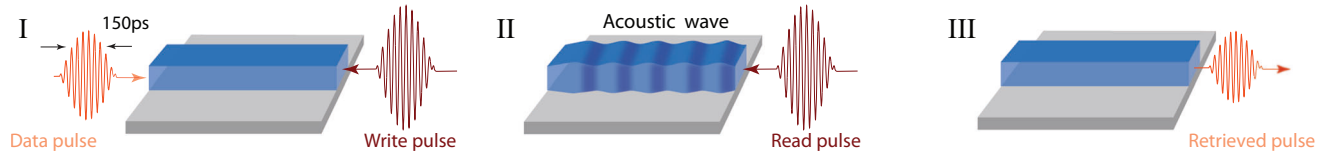
Fig. 1 | Principle of the Brillouin-based memory. (I) An optical data pulse of width 150 ps is depleted by a strong counter-propagating "write" pulse, storing the data pulse as an acoustic excitation (II). Retrieval process: a read pulse depletes the acoustic wave, converting the data pulse back to the optical domain (III).

mode equations for stimulated Brillouin interactions, (ii) the interference, mediated by the bandwidth of the optical pulse, with an additional acoustic mode, or (iii) manipulation of the optoacoustic interaction due to optical chirp or phase mismatch. We discuss the scale of these mechanisms and the experimental regimes where they become important. Achieving a delay for a record 15 ns at room temperature which corresponds to a delay of 100 pulse widths represents a steep improvement over previously published results which is enabled by the unique properties of the nonlinear chip that is used in this experiment. Although the underlying theory is well established, the possibility of such large delays for short pulses down to 150 ps was thought practically impossible, because the conditions have been difficult to achieve (e.g., minimizing the Raman gain cross-talk, high Brillouin gain during a short interaction time, compact footprint to minimize dispersion).

Results

To demonstrate the Brillouin interaction of optical pulses shorter than 1 ns, we use a Brillouin-based light storage setup, as shown in Fig. 1. A "data" pulse with central frequency $\omega_d/(2\pi)$ and a Full-Width at Half-Maximum (FWHM) pulse duration τ enters the Brillouin-active optical waveguide from one side. A counter-propagating "write" pulse, at the "control" frequency $\omega_c/(2\pi)$ down-shifted by the Brillouin frequency shift of $\Omega/(2\pi) = 7.7$ GHz, depletes the data pulse and excites a coherent acoustic wave in the optical waveguide. By sending in a "read" pulse at the control frequency $\omega_c/(2\pi)$, the acoustic wave is depleted and a retrieved optical data pulse propagates onwards in the original direction. (Note that here we avoid the conventional nomenclature of "pump" for the upper frequency and "Stokes" for the lower frequency laser pulses since in Brillouin storage experiments, the Stokes field has the higher intensity).

The first experimental results show the storage of 200 ps-long pulses (Fig. 2a). The data pulse can be retrieved from the acoustic wave after a storage time which is determined by the time difference between the write and read pulses. We achieved up to 14 ns delay while maintaining the pulse shape. The pulse width of the retrieved pulses for different storage times is shown in Fig. 2b, revealing an average pulse width of 230 ps, only slightly increased compared to the original data pulse. This indicates that our system preserves the pulse linewidth, while the storage time is still limited only by the acoustic lifetime. To further increase the capacity of the BBM, we encode eight different intensity levels on the original data pulse (Fig. 2c, left) which corresponds to 3 bits of information. We store and retrieve the different intensity levels after a storage time of 2 ns.

As shown in Fig. 2c (right panel), the intensity levels are almost perfectly retrieved, confirming that multiple bits of information can be stored (Fig. 2d).

In Fig. 3a, the same measurement is shown for 150 ps-long pulses, where the data can be retrieved up to 15 ns after the original pulse. This is a delay of 100 pulse widths, which is (to the best of our knowledge) a record for Brillouin-based memory.

Within this measurement series, we also encoded two amplitude levels on two consecutive short pulses to demonstrate the reliable retrieval of the respective levels and the maintenance of the bandwidth (Fig. 3b). Note that the storage of such short pulses is enabled by the large Brillouin gain in this type of chalcogenide waveguide, together with the high peak power of the control pulses. The criterion for efficient Brillouin storage is that the control pulse area be sufficiently large; the pulse area[20,26] is $\Theta = \sqrt{\pi c g_0 P_c/16 \ln 2\, n \tau_{ph} \tau_c}$ where $g_0 \sim 500\ \mathrm{m^{-1}\,W^{-1}}$ is the Brillouin gain,

$P_c \sim 20$ W is the peak power of the control pulse with pulse duration (FWHM) $\tau_c \sim 400$ ps, $n \sim 2.37$ is the optical mode index and $\tau_{ph} \sim 10$ ns is the phonon lifetime. With these values the pulse area is approximately $\Theta \sim 2.4$, which is not far from the optimum at $\Theta = \pi/2$, and yet not so strong that the "write" process begins to reverse, which occurs for $\Theta > \pi/2$. (This behavior is of course strongly analogous to the physics of the well-known optical Bloch equations[27]).

In the analysis of both measurements, we observed an anomalous aspect of the decay of the retrieved data pulses as compared to the normally observed exponential decay (corresponding to the exponential temporal decay of the acoustic wave). In Fig. 2a there is a smaller intensity than expected at 2 ns delay time. A similar behavior can be observed in Fig. 3a at delays of 2 ns and 6 ns. To determine that this was a genuine effect, we performed a more in-depth investigation of this oscillating read-out and studied the behavior of the delay and retrieval of pulses with durations of 280 ps, 440 ps, 760 ps, and 1 ns (see Fig. 4). In Fig. 4a, we observe a decay curve very close to exponential, but as the original data pulse becomes shorter, the departure from simple exponential decay becomes increasingly marked. For a pulse width of 280 ps and small steps in delay time, the minima and maxima in the read-out efficiency are very pronounced.

Discussion

In the Supplementary material we discuss three possible causes of this behavior. First, the pulse lengths in our experiments lie at the edge of the short pulse regime, where the usual slowly varying amplitude approximation breaks down[28]. For pulses below 200 ns, the Brillouin frequency would be imprinted in the read-out signal. Furthermore, simulations of the waveguide geometry revealed a secondary acoustic mode that could be excited during the writing process by the broad spectra of short optical pulses. The beating of two acoustic modes would result in oscillation in the read-out at their different frequency. However, pump-probe measurements of our waveguide did not show a secondary acoustic mode. Finally, alternative reasons might be considered to explain the oscillatory behavior. The electro-optic modulator could cause a chirp on the short pulses and the optical filters used to suppress residual pump light could cut into the broad spectrum of a short data pulse can induce significant dispersion on the filter edge. Alternatively, a detuning between the center frequency of the data and the write/read carrier relative to the Brillouin frequency shift might induce a beating. It is also worth noting, that the memory experiment in the short pulse regime was performed with longer write/read pulses compared to the data pulse which might explain some of the different behavior compared to previous experiments with longer pulses. None of the above explanations provides a full understanding of the measured oscillating behavior, warranting future investigation.

In conclusion, we have demonstrated stimulated Brillouin interactions with short pulses down to the 150 ps regime. With the concept of Brillouin-based memory, we showed that the limitations of the narrow Brillouin linewidth can be overcome by two orders of magnitude. Data pulses down to the 150 ps regime can be retrieved for up to 100 pulse widths while maintaining the pulse bandwidth, pulse shape, and amplitude encoded information.

Finally, we demonstrated a thorough measurement of the read-out intensity dependent on the storage time for different pulse widths which revealed an oscillating behavior. At this stage, the cause of this oscillatory behavior is not fully understood and requires further investigation.
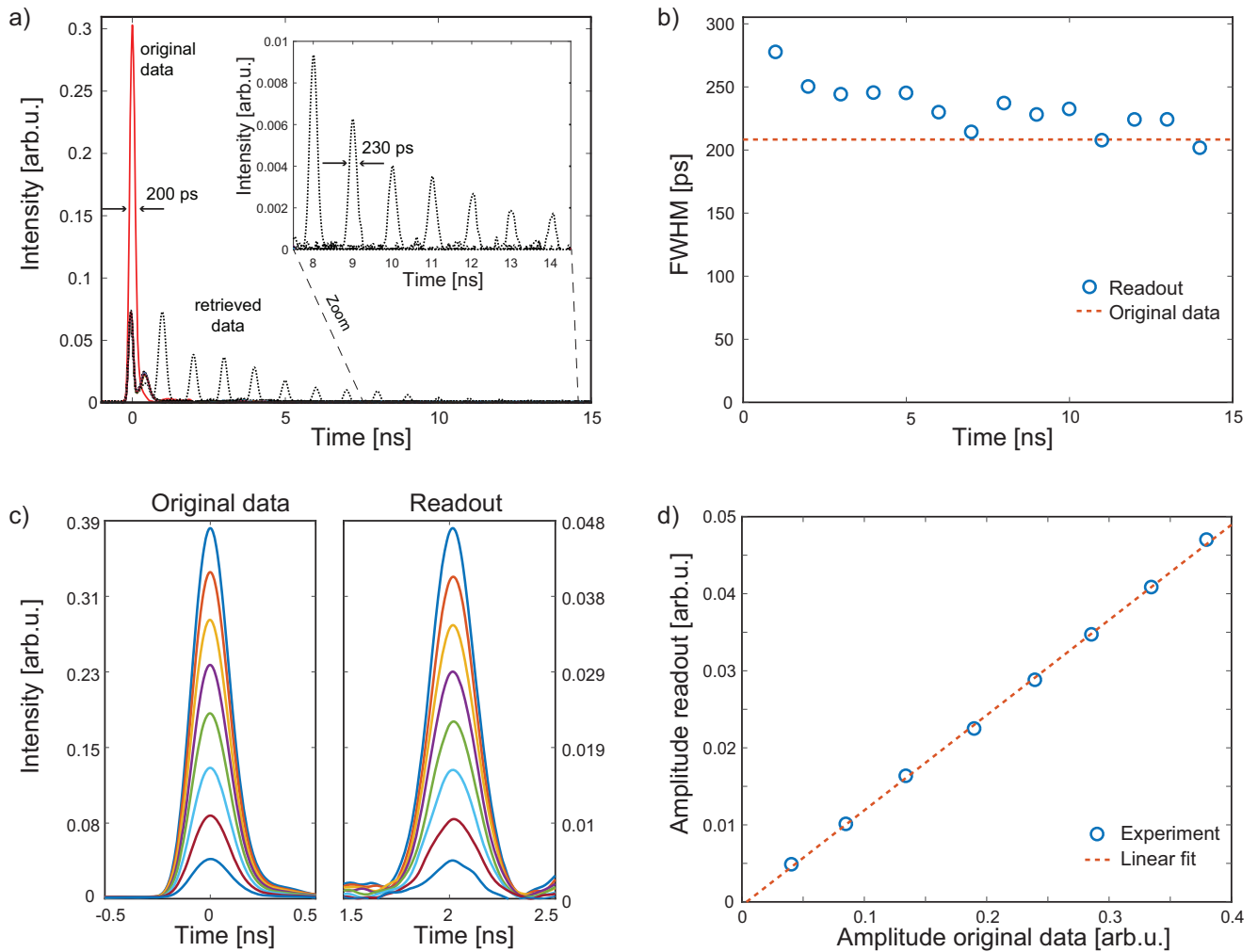
Fig. 2 | Experimental results. a Tunable storage of a 200 ps-long data pulse for up to 14 ns. The retrieved data is shown in black dotted lines. (The black signal shown with zero delay is the detected residual power of the data pulse that is not converted to the acoustic wave.) Inset: zoom-in from 8 to 14 ns. **b** Full-width at half-maximum of the retrieved pulses at different storage times, average value: 230 ps. **c** Read-out of different intensity levels after 2 ns. **d** Linear dependence of input to output amplitude.
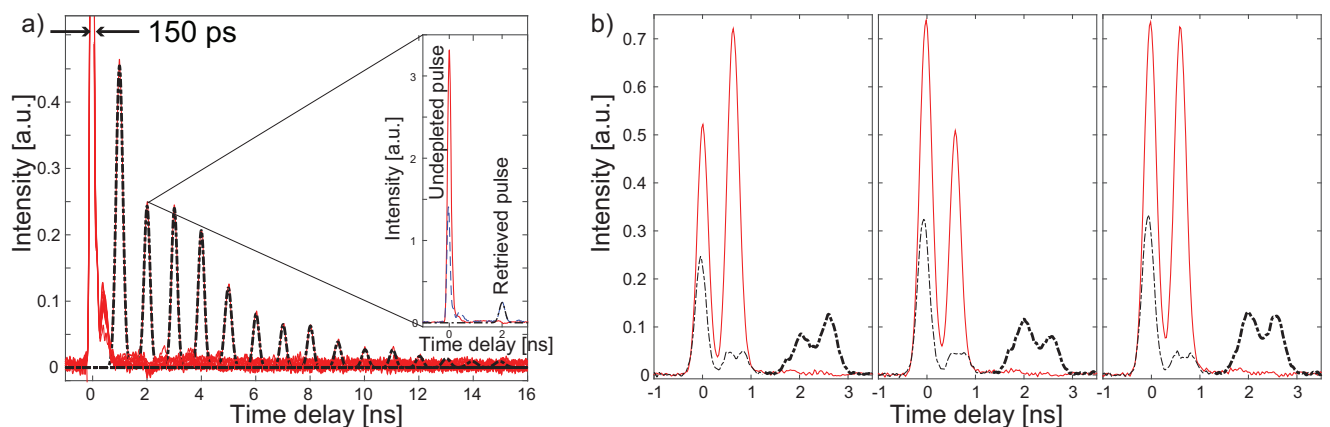
Fig. 3 | Experimental results. a 150 ps-long original data pulse (red) is stored for up to 15 ns (retrieved signals shown in black). The inset shows the undepleted pulse compared to the read-out pulse after 2 ns. **b** Two consecutive pulses with a pulse width of 280 ps and different amplitude levels are stored and retrieved after 2 ns. The pulse shape and amplitude levels for both optical pulses are retrieved. The detected signal with zero delay is due to the unconverted fraction of the input signal.
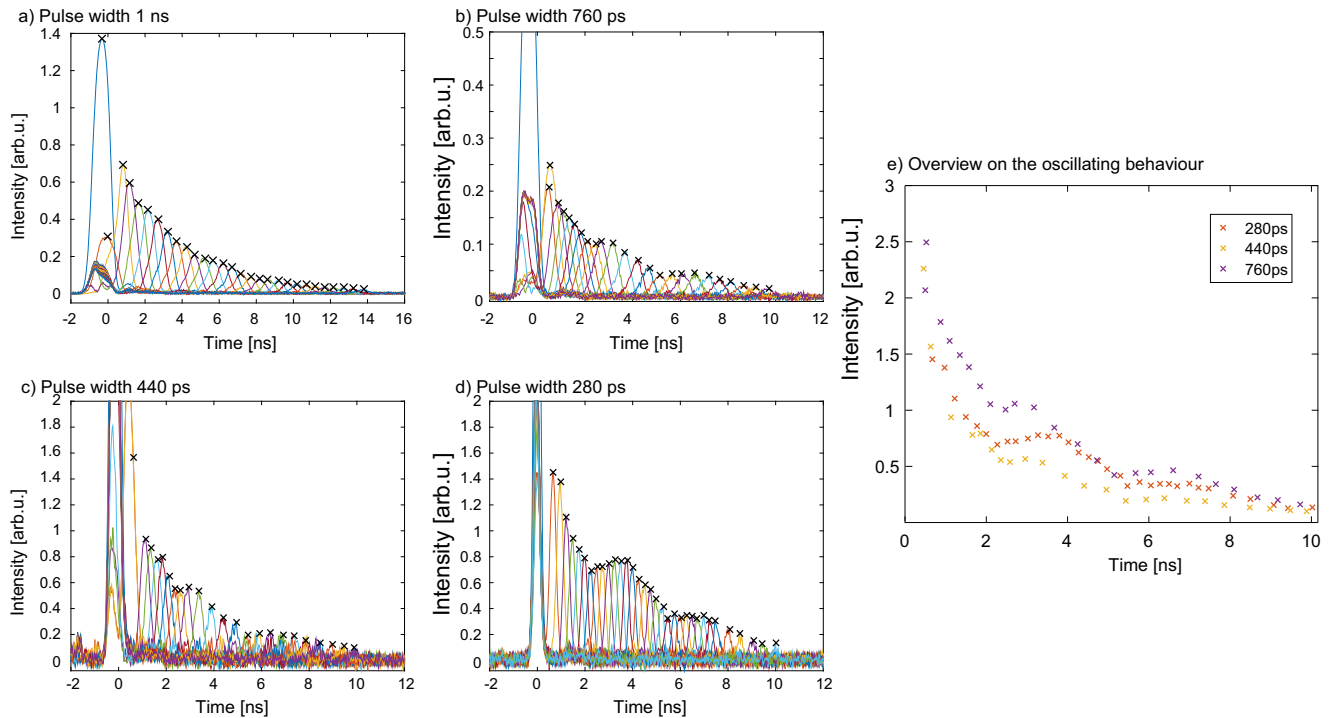
Fig. 4 | Experimental results. For comparison, the tunable storage of optical pulses with different pulse duration is shown: **a** 1 ns, **b** 760 ps, **c** 440 ps, and **d** 280 ps. **e** Overview of the oscillating behavior of the read-out amplitude: minima at delays of approximately 2.2 ns, 5.5 ns, and 9 ns can be observed.
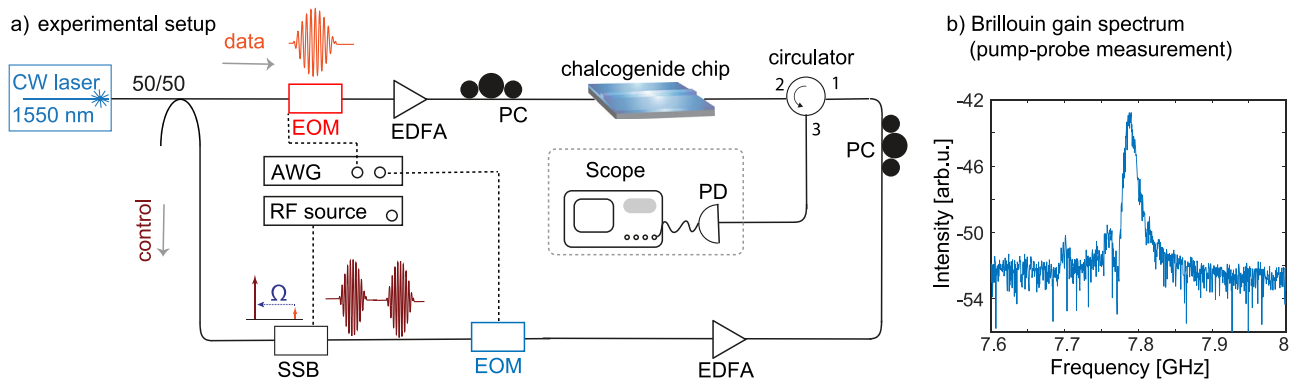

Fig. 5 | Experimental setup and typical Brillouin gain spectrum. a Brillouin-based memory setup. Components in the setup: EDFA erbium-doped fiber amplifier, PC polarization controller, SSB single-sideband modulator, EOM electro-optic modulator, PD photo diode, AWG arbitrary waveform generator, RF radio frequency. **b** Integrated Brillouin gain spectrum with a typical pump-probe continuous wave setup.

This work is a fundamental result representing a significant increase in Brillouin storage. We expect this work will stimulate other research to explore potential applications. We note that several key application areas can benefit from such storage: analog communications systems that use microwave photonics pulse manipulation[29], digital communication systems that rely on optical signal processing, and fiber-based Brillouin sensors that use optical pulses to achieve higher spatial resolution. Especially together with the previously shown coherence[20] and frequency-preserving nature of the Brillouin-based memory[21] it represents a versatile memory concept suitable for advanced coherent communication and processing schemes.

Methods

The experimental setup is depicted in Fig. 5. The output of a CW narrow-linewidth distributed feedback laser at 1550 nm is split into two arms: the data propagation part and the control pulses part. Data pulses with a pulse length down to $\tau = 150$ ps are generated by an electro-optic intensity

modulator and a high-speed arbitrary waveform generator. The data pulses are amplified and the polarization is adjusted for maximum transmission, before entering the photonic chip from one side with a coupled on-chip peak power ~50 mW. The As_2S_3 chalcogenide glass chip (which serves as the storage medium) contains a 17 cm-long small-footprint spiral waveguide with a cross-section of 2.2 μm × 0.850 μm. The propagation loss varies from 0.5 to 0.8 dB/cm. The Brillouin gain in these waveguides is typically in the order of 500 $m^{-1} W^{-1}$ [30]. The CW light on the control arm is frequency down-shifted by the Brillouin frequency shift $\Omega/(2\pi)$ via a single-sideband modulator driven by an RF source and the respective write and read pulses are imposed on the CW light using an intensity modulator and a second channel of the arbitrary waveform generator. After amplification, the read and write control pulses (coupled on-chip peak power ~20 W, Gaussians with pulse width 400 ps) enter the photonic waveguide from the opposite side (via port 1 of the circulator). We note that the power of the optical fields falls well below the computed Raman threshold of 113 W, and so Raman

scattering can be safely neglected. The retrieved data pulses exit at port 3 of the circulator before being filtered with a narrow-linewidth tunable filter Alnair ultra-narrow optical filter with minimum bandwidth of 3.7GHz and a filter roll-off of 1500 dB/nm and recorded in the time domain with a fast photodetector (New Focus 12 GHz IR Photoreceiver) and a fast oscilloscope (Keysight Infiniium 12 GHz High-Performance Oscilloscope).

Data availability

The measurement data is available from the authors by reasonable request.

References

1. Boyd, R. W. *Nonlinear Optics* (Acad. Press, 2003).
2. Merklein, M., Kabakova, I. V., Zarifi, A. & Eggleton, B. J. 100 years of Brillouin scattering: Historical and future perspectives. *Appl. Phys. Rev.* **9**, 041306 (2022).
3. Tanemura, T., Takushima, Y. & Kikuchi, K. Narrowband optical filter, with a variable transmission spectrum, using stimulated Brillouin scattering in optical fiber. *Opt. Lett.* **27**, 1552–1554 (2002).
4. Marpaung, D. et al. Low-power, chip-based stimulated Brillouin scattering microwave photonic filter with ultrahigh selectivity. *Optica* **2**, 76 (2015).
5. Choudhary, A. et al. Tailoring of the Brillouin gain for on-chip widely tunable and reconfigurable broadband microwave photonic filters. *Opt. Lett.* **41**, 436–439 (2016).
6. Sancho, J. et al. Dynamic microwave photonic filter using separate carrier tuning based on stimulated Brillouin scattering in fibers. *IEEE Photon. Technol. Lett.* **22**, 1753–1755 (2010).
7. Vidal, B., Piqueras, M. A. & Martí, J. Tunable and reconfigurable photonic microwave filter based on stimulated Brillouin scattering. *Opti. Lett.* **32**, 23–25 (2007).
8. Santagiustina, M., Chin, S., Primerov, N., Ursini, L. & Thévenaz, L. All-optical signal processing using dynamic Brillouin gratings. *Sci. Rep.* **3**, 1594 (2013).
9. Shin, H. et al. Control of coherent information via on-chip photonic-phononic emitter-receivers. *Nat. Commun.* **6**, 6427 (2015).
10. Song, K. Y., Lee, K. & Lee, S. B. Tunable optical delays based on Brillouin dynamic grating in optical fibers. *Opt. Exp.* **17**, 10344–10349 (2009).
11. Antman, Y., Levanon, N. & Zadok, A. Low-noise delays from dynamic Brillouin gratings based on perfect Golomb coding of pump waves. *Opt. Lett.* **37**, 5259–5261 (2012).
12. Eggleton, B. J., Poulton, C. G., Rakich, P. T., Steel, M. & Bahl, G. Brillouin integrated photonics. *Nat. Photon.* **13**, 664–677 (2019).
13. Hill, K. O., Kawasaki, B. S. & Johnson, D. C. cw Brillouin laser. *Appl. Phys. Lett.* **28**, 608 (1976).
14. Kabakova, I. V. et al. Narrow linewidth Brillouin laser based on chalcogenide photonic chip. *Opt. Lett.* **38**, 3208–3211 (2013).
15. Gundavarapu, S. et al. Sub-hertz fundamental linewidth photonic integrated Brillouin laser. *Nat. Photon.* **13**, 60–67 (2019).
16. Chauhan, N. et al. Visible light photonic integrated Brillouin laser. *Nat. Commun.* **12**, 4685 (2021).
17. Thévenaz, L. Slow and fast light in optical fibres. *Nat. Photon.* **2**, 474–481 (2008).
18. Zhu, Z., Gauthier, D. J. & Boyd, R. W. Stored light in an optical fiber via stimulated Brillouin scattering. *Science* **318**, 1748–1750 (2007).
19. Song, K. Y., Herráez, M. & Thévenaz, L. Observation of pulse delaying and advancement in optical fibers using stimulated Brillouin scattering. *Opt. Exp.* **13**, 82–88 (2005).
20. Merklein, M., Stiller, B., Vu, K., Madden, S. J. & Eggleton, B. J. A chip-integrated coherent photonic-phononic memory. *Natu. Commun.* **8**, 574 (2017).
21. Stiller, B. et al. Cross talk-free coherent multi-wavelength Brillouin interaction. *APL Photon.* **4**, 040802 (2019).
22. Merklein, M. et al. On-chip broadband nonreciprocal light storage. *Nanophotonics* **10**, 75–82 (2020).
23. Stiller, B. et al. On-chip multi-stage optical delay based on cascaded Brillouin light storage. *Opt. Lett.* **43**, 4321–4324 (2018).
24. Stiller, B. et al. Coherently refreshing hypersonic phonons for light storage. *Optica* **7**, 492–497 (2020).
25. Shapiro, S. L., Giordmaine, J. A. & Wecht, K. W. Stimulated Raman and Brillouin scattering with picosecond light pulses. *Phys. Rev. Lett.* **19**, 1093 (1967).
26. Dong, M. & Winful, H. G. Unified approach to cascaded stimulated Brillouin scattering and frequency-comb generation. *Phys. Rev. A* **93**, 043851 (2016).
27. Allen, L. & Eberly, J. *Optical Resonance and Two-Level Atoms*. Dover Books on Physics (Dover Publications, https://books.google.com.au/books?id=36DDAgAAQBAJ 2012).
28. Piotrowski, J., Schmidt, M. K., Stiller, B., Poulton, C. G. & Steel, M. J. Picosecond acoustic dynamics in stimulated Brillouin scattering. *Opt. Lett.* **46**, 2972–2975 (2021).
29. Varun, M. K., Mishra, A. & Pant, R. Microwave photonics applications of stimulated Brillouin scattering. *J. Opt.* **24**, 063002 (2022).
30. Choudhary, A. et al. Advanced integrated microwave signal processing with giant on-chip Brillouin gain. *J. Lightwave Technol.* **35**, 846–854 (2017).

Author contributions

B.S., K.J., and M.M. conceived the idea. B.S., K. J., and M. M. performed the experiments and analyzed the data. J.P., M.K.S., C.G.P., and M.J.K. developed the theory. K.V., P.M., and S.M. fabricated the sample. B.S., J.P., M.K.S., C.G.P., M.J.K., M.M., and B.J.E. wrote the manuscript with input from all authors.

Competing interests

The authors declare no competing interests.

Additional information

Supplementary information The online version contains supplementary material available at https://doi.org/10.1038/s44310-024-00004-x.

Correspondence and requests for materials should be addressed to Birgit Stiller.

Reprints and permissions information is available at http://www.nature.com/reprints

Publisher's note Springer Nature remains neutral with regard to jurisdictional claims in published maps and institutional affiliations.